

Microstructure evaluation of the Al-Ti alloy with magnesium addition

K. Labisz ^{a,*}, L.A. Dobrzański ^a, R. Maniara ^b, A. Olsen ^c

^a Division of Materials Processing Technology, Management and Computer Techniques in Materials Science, Institute of Engineering Materials and Biomaterials, Silesian University of Technology, ul. Konarskiego 18a, 44-100 Gliwice, Poland

^b TurboCare Poland S.A., ul. Powstańców Śląskich 85, 42-701 Lubliniec, Poland

^c Structural Physics, Centre for Materials Science, University of Oslo, Gaustadtalleen 21, N-0349 Oslo, Norway

* Corresponding author: E-mail address: krzysztof.labisz@polsl.pl

Received 06.05.2011; published in revised form 01.07.2011

Manufacturing and processing

ABSTRACT

Purpose: Effects of magnesium additions to Al alloy with 2% Ti addition on the microstructure, phase morphology and distribution and mechanical properties were investigated. Here are presented mainly microstructure changes after solution heat treatment concerning mainly grain uniformity and intermetallic phases of the aluminium – titanium alloy with a content of 2 and 4 % of magnesium addition. The purpose of this work was also to determine the solution heat treatment conditions of the investigation alloys.

Design/methodology/approach: The reason of this work was to determine the heat treatment parameters influence, particularly SHT temperature and time onto the changes of the microstructure of the investigated material, as well to determine which intermetallic phases occur after the heat treatment performed, and how is the particles morphology in as cast state compared to structure after heat treatment.

Findings: After solution heat treatment for 4 hours the structure changes in a significant way. The grains are larger and no more uniform as in the as cast state. The most stable intermetallic in the Al-Ti system is the Al₃Ti phase. The solution heat treatment time should be greater than 4 hours to ensure a proper solution of titanium and magnesium in the Al-α solid solution.

Research limitations/implications: The investigated aluminium samples were examined metallographically using optical microscope with different image techniques, scanning electron microscope and also analyzed using a Vickers micro-hardness tester, also EDS microanalysis was carried out.

Practical implications: As an implication for the practice an alloy can be developed with increased properties, which could be of great interest for the automotive or aerospace industry. There are existing many different investigation areas and the knowledge found in this research shows one of interesting investigation direction.

Originality/value: The combination of light weight and high strength achieved in the Al-Ti alloys is very attractive for aerospace and automotive industries. Addition of magnesium into the Al-Ti alloy could help also to reveal the existence new unknown phases.

Keywords: Casting; Heat treatment; Aluminium alloys; Magnesium

Reference to this paper should be given in the following way:

K. Labisz, L.A. Dobrzański, R. Maniara, A. Olsen, Microstructure evaluation of the Al-Ti alloy with magnesium addition, Journal of Achievements in Materials and Manufacturing Engineering 47/1 (2011) 75-82.

1. Introduction

As all materials, aluminium alloys have an advantages and disadvantages. Their advantages include first of all: low density, relatively high specific strength, good castability, and good weldability in a controlled atmosphere, good corrosion resistance.

The most important disadvantages are: low Young's modulus, limited possibilities of cold workability, relatively low hardness, limited strength and creep resistance at elevated temperatures, high chemical reactivity, in some cases, limited corrosion resistance. The titanium-aluminium binary system provides a model for solution strengthening. In addition, it is the prototype of technical α alloys, as well as the α components of $\alpha+\beta$ alloys [1-8].

Aluminium is the most widely used alloying element in titanium-based alloys for example in the automobile or sport industry (Figs. 1a and b). It is the only common metal that raises the beta transus temperature and have large solubilities in both the alpha and beta phases. On the basis of theoretical considerations, deviations may arise from the fact that size parameters gradually reach the dimensions of some characteristic lengths related to the original deformation mechanism, e.g. the width of a dislocation source in the case of glide deformation. Under these circumstances, additional constraints may complicate or impede single steps of the formerly prevailing deformation mode, thus contributing to changes in the mechanical behaviour [9-18].

a)



b)



Fig. 1. Elements for the car and sport industry produced from the Al-Ti alloy, a) car wheel, b) bicycle equipment

The possibility of establishing thermally stable fine-scale dispersion of secondary phases in the as-quenched structure or during subsequent heat treatment offers potential improvement in mechanical properties of alloys via this route. Al-based alloys are particularly suitable to be developed by solution heat treatment and ageing, but only nine elements show appreciable solid solubility (greater than 1 at. %) in Al and only five of these have been exploited commercially [19-24].

Magnesium was used as the alloying additive, because it:

- the aspect ratio (length/width) of precipitates changed to higher values (e.g. above 3),
- reduces agglomeration of phases particles,
- increases porosity.

Apart from the alpha and beta phases, the presence of Ti_3Al phase (known as α_2) and $TiAl$ (gamma) intermetallic phase in the titanium-aluminium binary system is also noteworthy (Fig. 2). Both phases are of great technical importance (e.g., titanium-aluminide alloys, important for high-temperature applications). Also the occurrence of small amount of the magnesium titanium $Al_{18}Mg_3Ti_2$ phase could be expected (Fig. 3). Of great importance is also nano- and submicrocrystalline alloy microstructure characterised by high values of strength and hardness. Many studies have addressed the question of to what can be performed practical to implement this Hall-Petch behaviour, entailing a correlation between yield strength (σ_y) and grain size (d) according to this dependence [25-29].

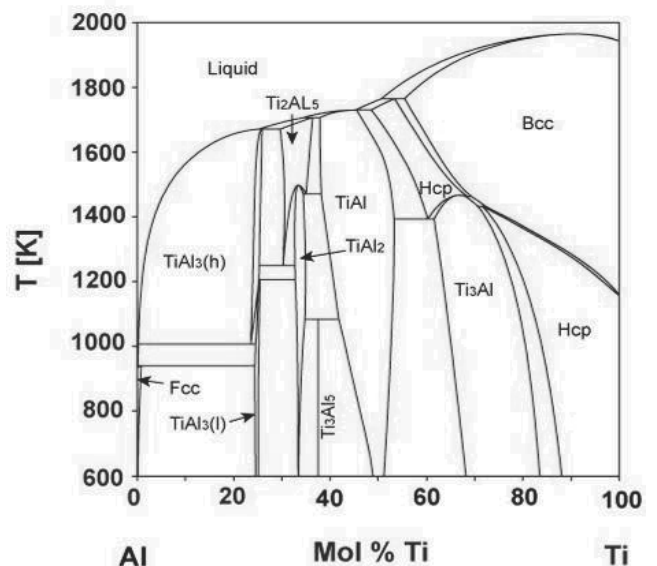


Fig. 2. Al-Ti phase diagram

In this work the $TiAl_3$ phase is of great interest which is an ordered structure based on the hexagonal close-packed alpha phase. A unit cell of the DO19 structure is composed of four regular HCP cells supported by covalent-like directional bonds connecting the titanium and aluminium atoms. [30-34].

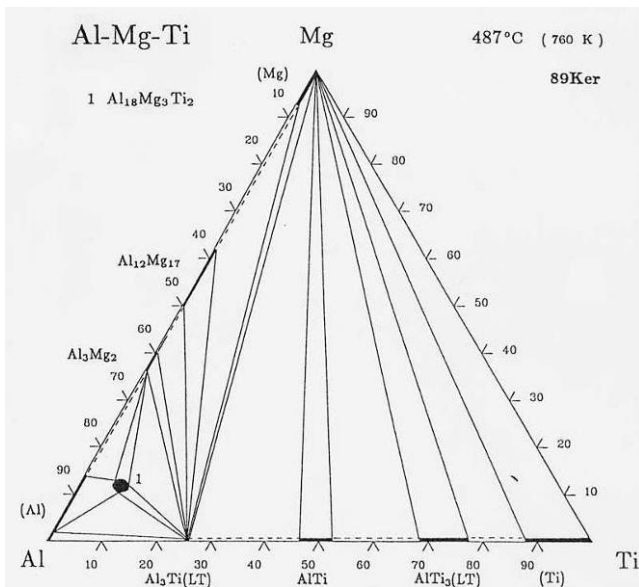


Fig. 3. Al-Ti-Mg ternary phase diagram

2. Experimental procedure

The alloys used for this work were produced in the SINTEF laboratory, with the basic components of Al 99.99%, Ti 99.99%, Mg 99.99% and basic alloy 10 Ca Al (R2516), incl.: Ca 9.33%, Fe 0.08%, Si 0.01%, Mg 0.06%, Sr 0.014% (wt%) like impurities.

It is an experimental aluminium-titanium alloy with magnesium addition which was investigated in this work. The exact chemical composition is showed in Table 1. Using a properly adjusted (Fig. 4) electro-resistance furnace all elements with the calculated and measured amount of the additives were melted in a ceramic crucible and then melt into a carbon form, witch was cooled in air in a water-cooled aluminium block. In the furnace a controlled protective argon atmosphere was used to avoid contamination and oxidation of molten aluminium and additives.

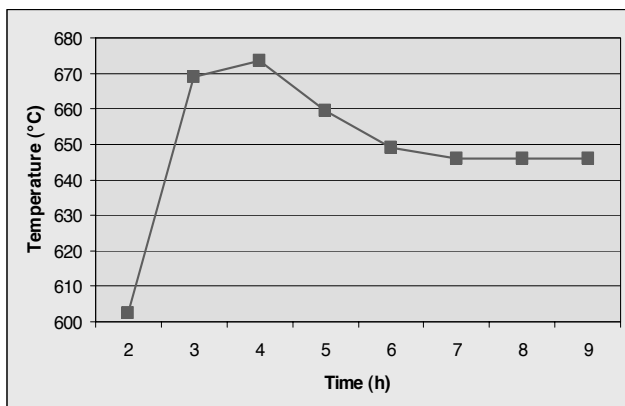


Fig. 4. Furnace temperature adjustment diagram

Samples with masses of approximately 120 ± 20 g were melted in a carbon mould. Than the mould with liquid metal was located in a water-cooled aluminium radiator. Cooling rate during the solidification was in range $1.6\text{-}2.5^\circ\text{C/s}$ - depending of the kind of alloy investigated. Samples for analysis of the microstructure were cute close to the centre of the cast samples. The cross sections of the specimen were ground, polished (used slurry up to $1 \mu\text{m}$) and anodized in HBF₄ acid water solution for grain, microstructure and phase observation. The microstructure of the samples were observed by an light microscope provided by Richter-Jung, model MEF3 LOM computerised with special KS 300 software.

It was very important to keep a high purity of the raw materials. It was chosen a 99.99% Al and 99.99% Ti master alloy which was the highest purity industrially available. Special care has also been taken in the melting and casting process: an alumina and a graphite crucible made from a high purity material was used, together with argon of 99.9999% purity to avoid contamination by gas elements, especially hydrogen.

For identification of the phases Scanning Electron Microscope equipped with EDS detector, Transition Electron Microscope (TEM) 200Cx supplied by Joel was used. The sample for TEM were ground mechanical to below a value in the range of 25 to 50 μm in thickness and 3 mm disk-diameter, and than thinned electrolytic at 40-50 volt, with 3 ampere current in T4 electrolyte for 20 s.

Table 1.

Chemical composition of the investigated alloys in wt. %

Alloy	Al	Ti	Mg
AlTi2Mg2	96	2	2
AlTi2Mg4	94	2	4

Qualitative and quantitative assessment of the chemical compositions of the phases was investigated using Philips XL 200 scanning microscope with energy dispersive spectrometer. For each phase about 8 separate spot measurements were made and also statistical values like mean values were calculate.

The microhardness was measured using a HV hardness testing machine supplied by Zwick, with HV_{0.05} scale. The microhardness was measured in 8 places and the a mean value was calculated.

3. Results and discussion

3.1. Microstructure characterization of the alloy in as cast state

The microstructure investigations reveals that after casting in the as-cast the alloy microstructure is non-uniform with areas of very small grains and some big grains inside (Fig. 5). There is a small amount of the Al₃Ti phase. This Al₃Ti phases particles are formed in localized regions of the matrix, and they do not

suppress the growth of directional pores in the other regions. Spherical pores surrounded by equiaxed peritectic microstructure and homogeneously distributed Al_3Ti phases are formed, because the primary α -Al and Al_3Ti phases probably prevent the growth of directional pores. These Al_3Ti phase particles could be observed in the optical micrographs presented on Figs. 6a-c. Titanium phase Al_3Ti showed on this figures is present in form of bulk particles over the whole structure, as well in form of longitudinal needle in case of both investigated alloys AlTi_2Mg_2 and AlTi_2Mg_4 .

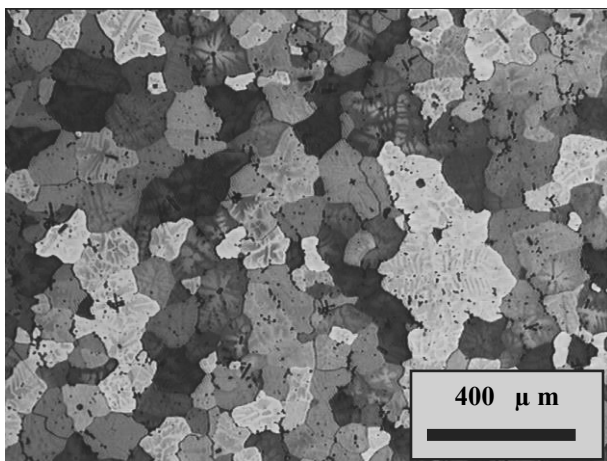


Fig. 5. Microstructure of the Al-Ti-Mg alloy in as cast state

3.2. Solution heat treatment performed on the AlTi_2Mg_2 and AlTi_2Mg_4 alloy

Heat treatment of the investigated alloys includes two following steps: solution heat treatment and artificial aging. In this paper there is especially investigated the microstructure after properly performed solution heat treatment. The heat treatment was performed in an electrical resistance furnace, and the samples were cooled in water. Temperature of solution heat treatment was determinate experimental, using a pair of thermocouples place inside the furnace. The applied SHT time was 24 hours. Artificial aging was performed in 180°C for 30, 60, 120 and 240 min also in an electrical resistance furnace, after this operation samples were cooled in air slowly.

To establish the highest possible solution heat treatment temperature, the samples were heat treated also in higher temperature above 600°C until small areas with partial melting places were detected. So in finally a temperature of 580°C and 575°C - Table 2 - was determined as the highest possible. Furthermore structural changes were find in samples with different time of solution heat treatment compared to the structure of as cast alloy. Generally grain growth can be state according to the selected time.

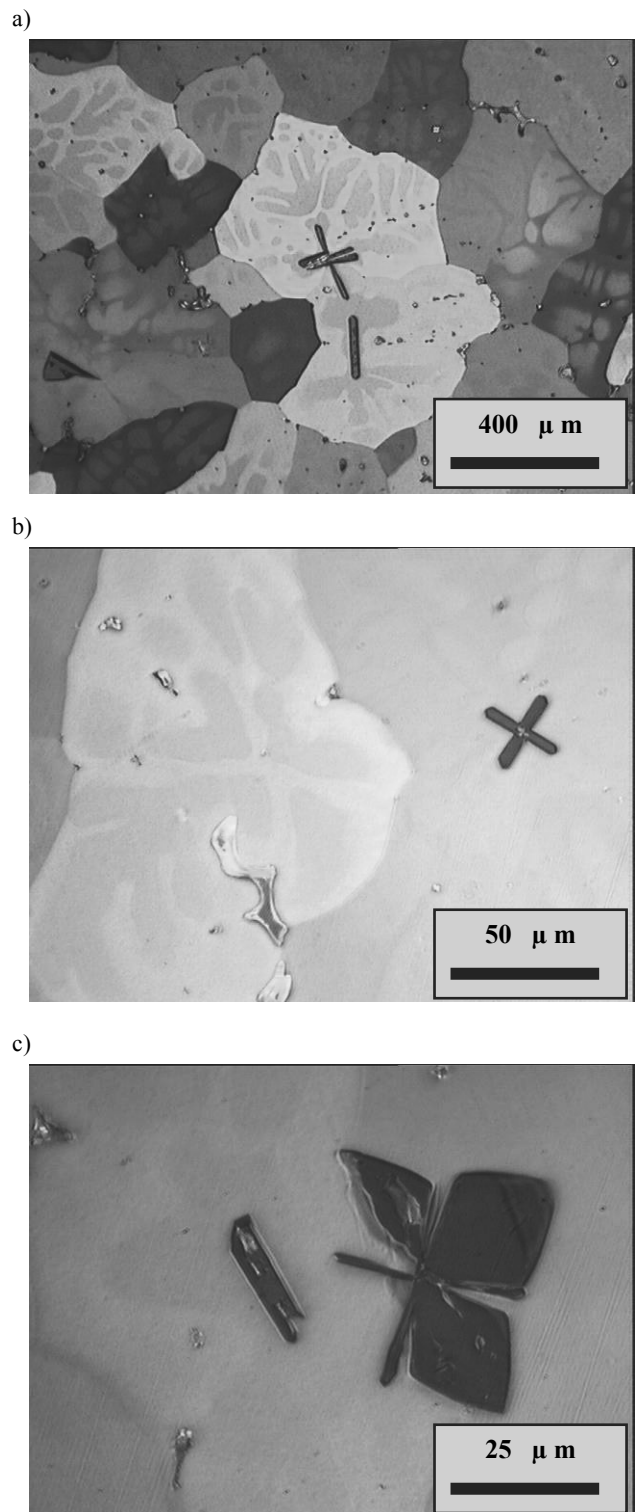


Fig. 6. Microstructure of the Al-Ti-Mg alloy in as cast state, a) dendritic character of the grain chemical composition, b) longitudinal Al_3Ti phase, c) bulk shaped Al_3Ti phase

Table 2.

Temperature applied for the of solution heat treatment for the investigated alloys

Alloy	Solution Heat Treatment temperature, °C
AlTi2Mg2	580±1
AlTi2Mg4	575±1

Form the investigate alloys also hardness was measurement was performed in the Vicker HV_{0.05} scale. The results are presented in Table 3 for the as cast material as well for solution heat treatment performed for 4 hours.

Table 3.

Vickers microhardness HV_{0.05} measurements results of the investigated AlTi2Mg2 AND AlTi2Mg4 alloys

Alloy	Heat treatment		Hardness, HV _{0.05}	
	As cast state	After SHT for 4 hours	As cast state	After SHT for 4 hours
AlTi2Mg2	52±1	27±1	52±1	27±1
AlTi2Mg4	58±1	52±1	58±1	52±1

In general the microstructure of the AlTi2Mg4 reveals smaller grains compared to the AlTi2Mg2 alloy (Fig. 11 and Fig. 14). The chemical composition dendrite-like non-homogeneity inside the grains is also less visible in case of the AlTi2Mg4 alloy (Figs. 12 and 15). For both of the alloys there is the Al₃Ti phase discovered, (Figs. 7-10), but for the AlTi2Mg2 alloy (Fig. 13) it is present in form of bulk shaped form, where as for the AlTi2Mg4 is appears mainly in the bulk and longitudinal needle form (Fig. 16).

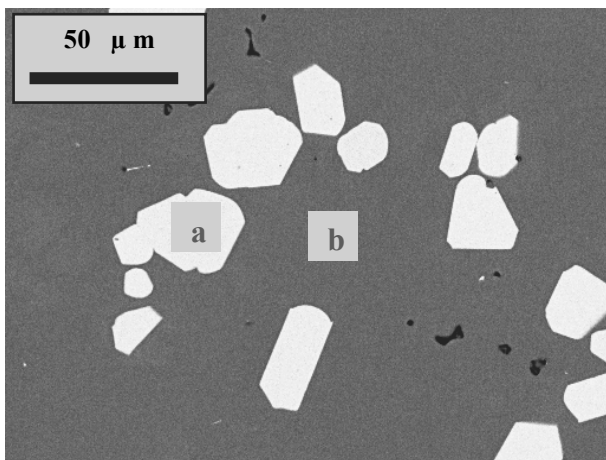


Fig. 7. SEM microstructure for EDS microanalysis performed on visible phase particles AlTi2Mg2 alloy

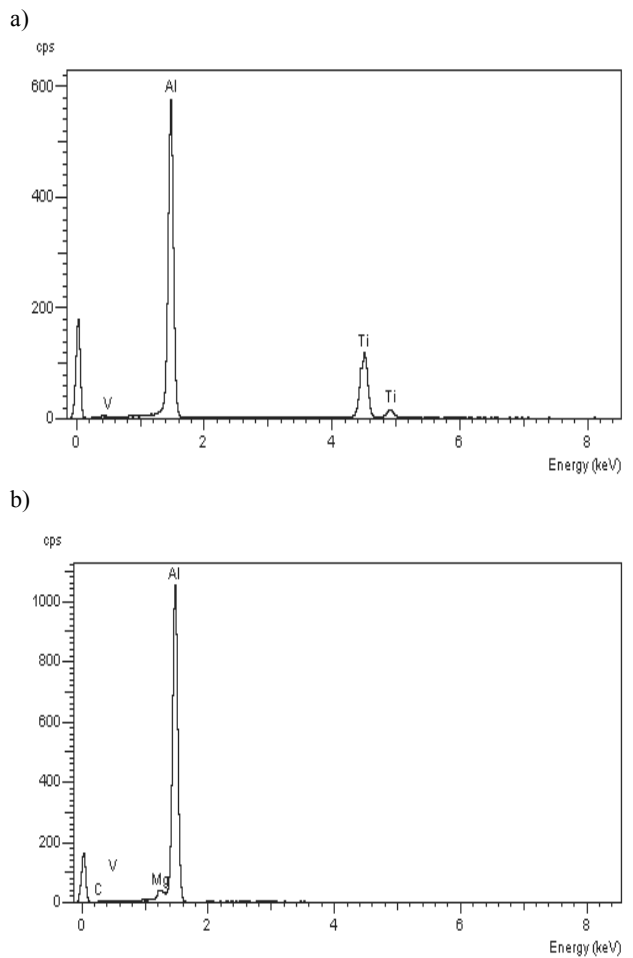


Fig. 8. EDS microanalysis performed on the marked places (a, b) on Fig. 7, AlTi2Mg2 alloy

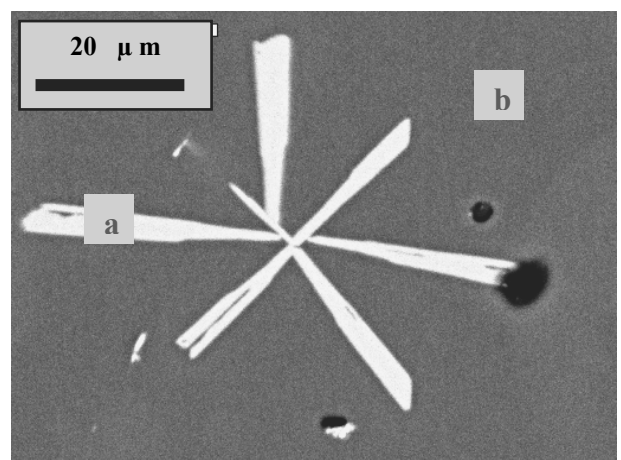


Fig. 9. SEM microstructure for EDS microanalysis performed on visible phase particles AlTi2Mg4 alloy

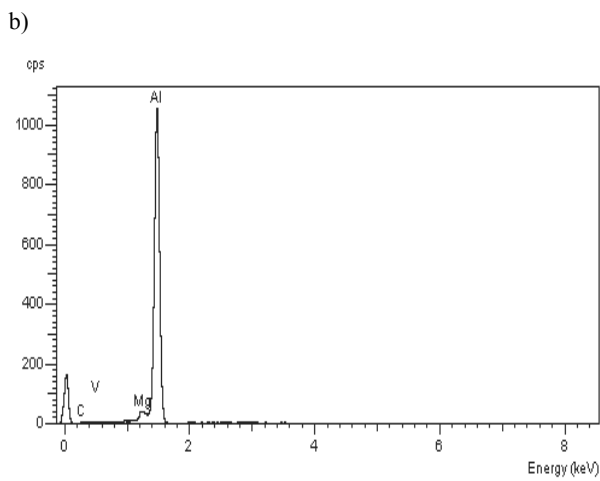
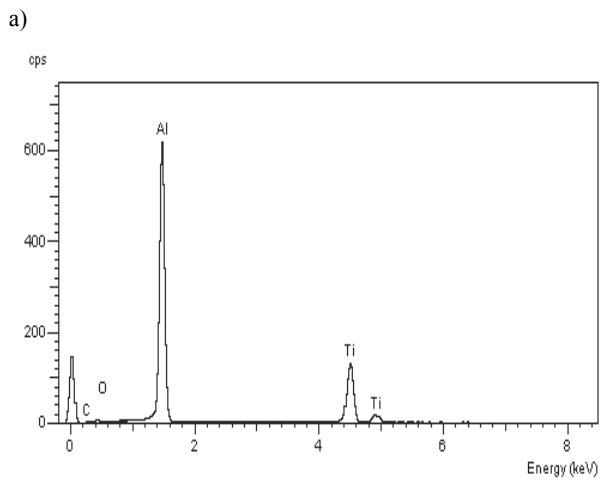


Fig. 10. EDS microanalysis performed on the marked places (a, b) on Fig. 9, AlTi2Mg4 alloy

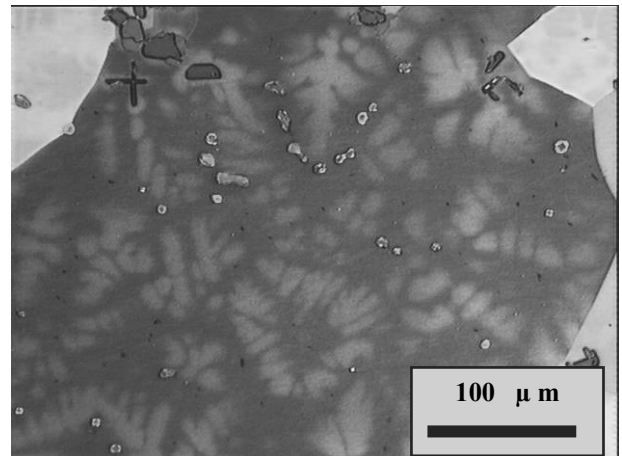


Fig. 12. Differences in chemical composition in a grain of the AlTi2Mg2 alloy after SHT in 580°C for 4 h

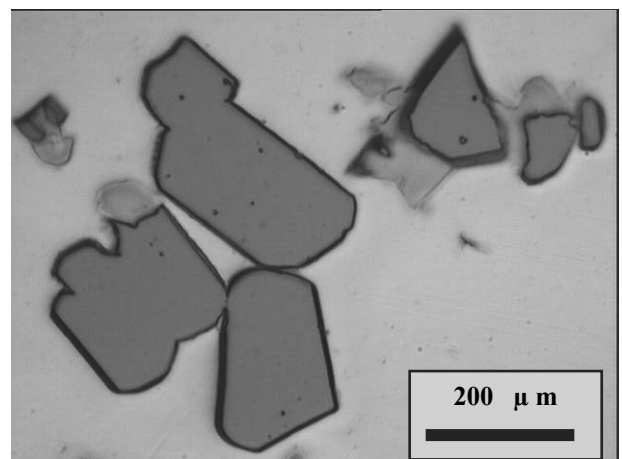


Fig. 13. Al₃Ti phase morphology, AlTi2Mg2 alloy after SHT in 580°C for 4 h

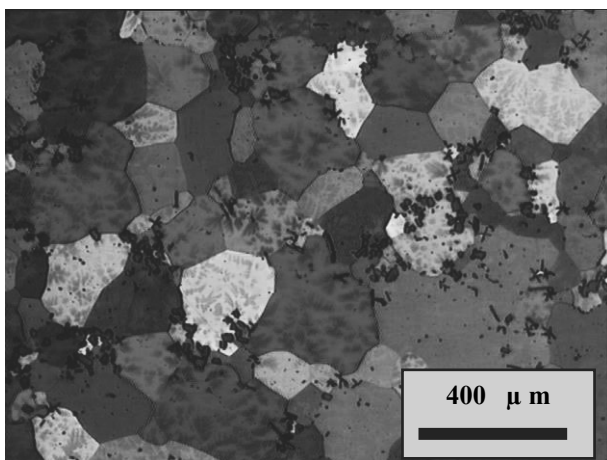


Fig. 11. Grain size of the AlTi2Mg2 alloy after SHT in 580°C for 4 h

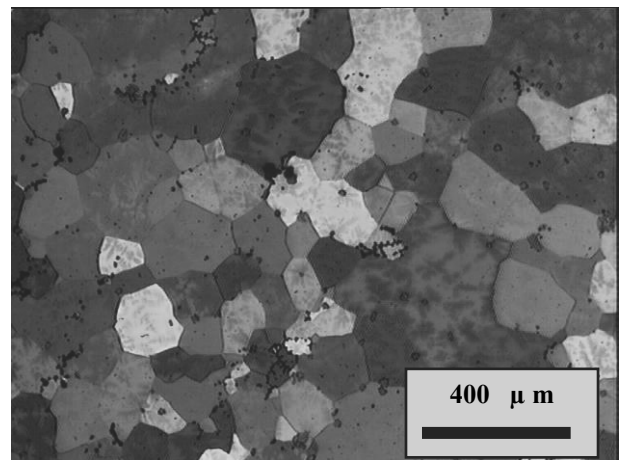


Fig. 14. Grain size of the AlTi2Mg4 alloy after SHT in 575°C for 4 h

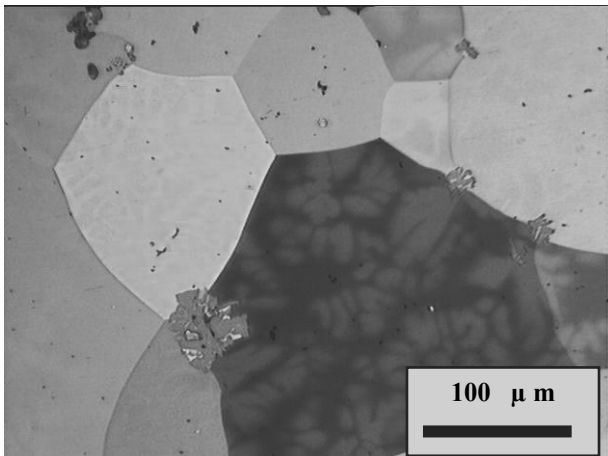


Fig. 15. Differences in chemical composition in a grain of the AlTi2Mg4 alloy after SHT in 575°C for 4 h

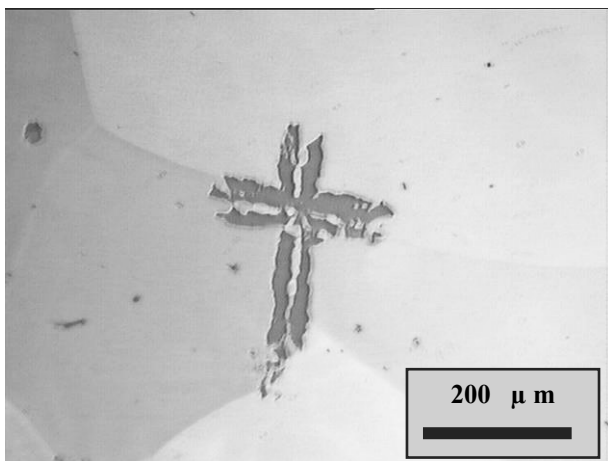


Fig. 16. Al₃Ti phase morphology, AlTi2Mg4 alloy after SHT in 575°C for 4 h

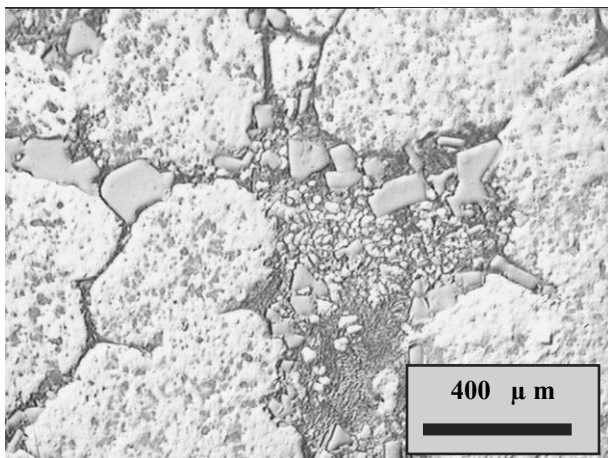


Fig. 17. Partially melting areas

4. Conclusions

It could be found on the basis of the microstructure investigations that directly after casting the as-cast alloy is non-uniform with areas of very small grains and some big grains inside. After solution heat treatment at the temperature of 580°C (AlTi2Mg2 alloy) and 575°C (AlTi2Mg4 alloy) for 4 hours the structure changes in a way, that the grains are larger for both alloys (Figs. 11 and 14) and no more uniform as revealed in the as cast state. This process is continuing also for a longer solution heat treatment time. Both in the as cast state and after SHT process the Al₃Ti phase can be observed. With a higher SHT temperature - when partially melting areas occur (Fig. 17) as well with a longer SHT time the Al₃Ti phase is growing up and breaking up in smaller parts. With a higher temperature a small amount of titanium (coming from the particles) is going into the solution (Al- matrix).

This process is confirmed with the hardness measurements where after 4 h solution heat treatment 27 HV_{0.05} (AlTi2Mg2 alloy) and 52HV_{0.05} (AlTi2Mg4 alloy) is measured, compared to 58 and 52HV_{0.05} respectively. So the hardness value decreases for this alloy below the value of as-cast alloy (Fig. 18). But with an increase of the magnesium content ten hardness increases, that could be a reason for further investigations of this alloy with a higher Mg content. The reason for that can be, that the chemical composition gradient inside the grain changes and so the strengthening effect decreases.

We can conclude also that:

- The most stable intermetallic phase in the investigated Al-Ti system is the Al₃Ti phase,
- A proper solution heat treatment time of 4 hours is too short for maximising the mechanical properties of these alloys.

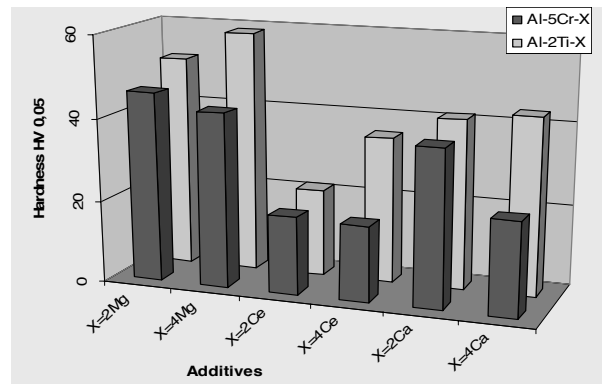


Fig. 18. Hardness measurements results of the alloys with magnesium, cerium and calcium addition

Acknowledgements

The authors would like to express his great thanks to the Center of Materials Science, especially to the Structural Physics group for great help and scientifically support in elaboration of this project. The authors are especially grateful to Mr Przemysław Zagierski and Mr Eric Sörbredén for his valuable support and very usefully comments and assistance in preparing of the investigation.

References

- [1] K. Labisz, M. Krupiński, L.A. Dobrzański, Phases morphology and distribution of the Al-Si-Cu alloy, *Journal of Achievements in Materials and Manufacturing Engineering* 37/2 (2009) 309-316.
- [2] L.A. Dobrzański, K. Labisz, R. Maniara, A. Olsen, Microstructure and mechanical properties of the Al-Ti alloy with cerium addition, *Worldwide Journal of Achievements in Materials and Manufacturing Engineering* 37/2 (2009) 622-629.
- [3] J. Djuricic, S. Boro, G. Pickering, P. Stephen, Nanostructured cerium oxide: preparation and properties of weakly-agglomerated powders, *Journal of the European Ceramic Society* 19/11 (1999) 1925-1934.
- [4] D.Y. Maeng, J.H. Lee, S.I. Hong, The effect of the transition elements on the superplastic behavior of Al-Mg alloys, *Materials Science and Engineering* 357/1-2 (2003) 188-195.
- [5] M. Beschliesser, H. Clemens, H. Kestler, F. Jeglitsch, Phase stability of a c-TiAl based alloy upon annealing: comparison between experiment and thermodynamic calculations, *Scripta Materialia* 49 (2003) 279-284.
- [6] K. Ozturuk, L.Q. Chen, Z.K. Liu, Thermodynamic assessment of the Al-Ca binary system using random solution and associate models, *Journal of Alloy and Compounds* 340/1-2 (2003) 199-206.
- [7] J. Szajnar, T. Wróbel, Inoculation of primary structure of pure aluminium, *Journal of Achievements in Materials and Manufacturing Engineering* 20 (2007) 283-286.
- [8] P. Villars, A. Prince, H. Okamoto, *Handbook of Ternary Alloy Phase Diagram*, vol. IV, ASM, 1995.
- [9] M. Krupiński, K. Labisz, Z. Rdzawski, M. Pawlyta, Cooling rate and chemical composition influence on structure of Al-Si-Cu alloys, *Journal of Achievements in Materials and Manufacturing Engineering* 45/1 (2011) 13-22.
- [10] P.L. Schaffer, A.K. Dahle, Settling behaviour of different grain refiners in aluminium, *Materials Science and Engineering* 413-414 (2005) 373-378.
- [11] P. Villars, L.D. Cavert, *Pearson's handbook of crystallographic data for intermetallic phases*, vol. 2, ASM, 1991.
- [12] T. Tański, K. Labisz, L.A. Dobrzański, Effect of Al additions and heat treatment on corrosion properties of Mg-Al based alloys, *Journal of Achievements in Materials and Manufacturing Engineering* 44/1 (2011) 64-72.
- [13] M. Krupiński, K. Labisz, L.A. Dobrzański, Z. Rdzawski, Image analysis used for aluminium alloy microstructure investigation, *Journal of Achievements in Materials and Manufacturing Engineering* 42 (2010) 58-65.
- [14] M. Krupiński, K. Labisz, L.A. Dobrzański, Z. Rdzawski, Computer aided microstructure analysis of the Al-Si-Cu cast alloy cooled with different cooling rates, *Proceedings of the 13th "International Materials Symposium" IMSP'2010, Denizli, 2010, 724-730.*
- [15] M. Krupiński, K. Labisz, L.A. Dobrzański, Z. Rdzawski, Derivative thermo-analysis application to assess the cooling rate influence on the microstructure of Al-Si alloy cast, *Journal of Achievements in Materials and Manufacturing Engineering* 38/2 (2010) 115-122.
- [16] Y. Han, D. Shu, J. Wang, B. Sun, Microstructure and grain refining performance of Al-5Ti-1B masteralloy prepared under high-intensity ultrasound, *Materials Science and Engineering A* 430 (2006) 326-331.
- [17] L.A. Dobrzański, K. Labisz, R. Maniara, Microstructure investigation and hardness measurement in Al-Ti alloy, *Proceedings of the 13th Scientific International Conference „Achievements in Mechanical and Materials Engineering” AMME'2005, Zakopane, 2005, 161-166.*
- [18] X. Wang, A. Jha, R. Brydson, In situ fabrication of Al₃Ti particle reinforced aluminium alloy metal-matrix composites, *Materials Science and Engineering A* 364 (2004) 339-345.
- [19] V. Maurice, G. Despert, S. Zanna, P. Josso, M.-P. Bacos, P. Marcus, XPS study of the initial stages of oxidation of a₂-Ti₃Al and c-TiAl intermetallic alloys, *Acta Materialia* 55 (2007) 3315-3325.
- [20] L.A. Dobrzański, M. Król, T. Tański, Effect of cooling rate and aluminum contents on the Mg-Al-Zn alloys' structure and mechanical properties, *Journal of Achievements in Materials and Manufacturing Engineering* 43 (2010) 613-633.
- [21] G. Mrówka-Nowotnik, J. Sieniawski, M. Wierzbńska, Intermetallic phase particles in 6082 aluminium alloy, *Archives of Materials Science and Engineering* 28 (2007) 69-76.
- [22] L.A. Dobrzański, K. Labisz, A. Olsen, P. Zgierski, Precipitation processes during heat treatment of the Al-Mg-Cu-Zn alloy for car chassis, *Proceedings of the 10th Jubilee Scientific International Conference „Achievements in Mechanical and Materials Engineering” AMME'2001, Zakopane, 2001, 645-650 (in Polish).*
- [23] P. Švančárek, D. Galusek, F. Loughran, A. Brown, R. Brydson, A. Atkinson, F. Riley, Microstructure-stress relationships in liquid-phase sintered alumina modified by the addition of 5 wt.% of calcia-silica additives, *Acta Materialia* 54 (2006) 4853-4863.
- [24] L.A. Dobrzański, M. Krupiński, K. Labisz, B. Krupińska, A. Grajcar, Phases and structure characteristics of the near eutectic Al-Si-Cu alloy using derivative thermo analysis, *Materials Science Forum* 638-642 (2010) 475-480.
- [25] L.F. Mondolfo, *Aluminium alloys structure and properties*, Butterworths, London, 1976.
- [26] P. Ashraf, P. Muhamed, S.M.A. Shibli, Development of cerium oxide and nickel oxide-incorporated aluminium matrix for marine applications, *Journal of Alloys and Compounds* 484/1-2 (2009) 477-482.
- [27] C. Weiping, Diffusion of cerium in the aluminium lattice, *Journal of Materials Science Letters* 16/22 (1997) 1824-1826.
- [28] A. Pardo, S. Feliú, M.C. Merino, R. Arrabal, E. Matykina, The effect of cerium and lanthanum surface treatments on early stages of oxidation of A361 aluminium alloy at high temperature, *Applied Surface Science* 254/2 (2007) 586-595.
- [29] A. de Frutos, M.A. Arenas, Y. Liu, P. Skeldon, G.E. Thompson, J. de Damborenea, A. Conde, Influence of pre-treatments in cerium conversion treatment of AA2024-T3 and 7075-T6 alloys, *Surface & Coatings Technology* 202 (2008) 3797-3807.
- [30] M.F. Montemor, A.M. Simões, M.J. Carnezim, Characterization of rare-earth conversion films formed on the AZ31 magnesium alloy and its relation with corrosion protection, *Applied Surface Science* 253/16 (2007) 6922-6931.
- [31] T. Dhannia, S. Jayalekshmi, M.C. Santhosh Kumar, T. Prasada Rao, A. Chandra Bose, Effect of aluminium doping and annealing on structural and optical properties of cerium oxide nanocrystals, *Journal of Physics and Chemistry of Solids* 70/11 (2009) 1443-1447.
- [32] A. Decroly, C. André, J. Petitjean, J. Jean-Pierre, Study of the deposition of cerium oxide by conversion on to aluminium alloys, *Surface and Coatings Technology* 194/1 (2005) 1-9.
- [33] A. Włodarczyk-Fligier, M. Adamiak, L.A. Dobrzański, Corrosion resistance of the sintered composite materials with the EN AW-AlCu4Mg1(a) alloy matrix reinforced with ceramic particles, *Journal of Achievements in Materials and Manufacturing Engineering* 42 (2010) 120-126.
- [34] L.A. Dobrzański, M. Kremzer, A.J. Nowak, A. Nagel, Aluminium matrix composites fabricated by infiltration method, *Archives of Materials Science and Engineering* 36/1 (2009) 5-11.